

Supporting Information for

A New Strategy to Develop Superior Electrode Materials for Advanced Batteries: Using Positive Cycling Trend to Compensate the Negative One to Achieve Ultralong Cycling Stability

Dai-Huo Liu,^{§a} Hong-Yan Lü,^{§a} Xing-Long Wu,^{*a} Jie Wang,^a Xin Yan,^a Jing-Ping Zhang,^a
Hongbo Geng,^b Yu Zhang,^b and Qingyu Yan^{*b}

^a National & Local United Engineering Laboratory for Power Batteries, Department of Chemistry, Northeast Normal University, Changchun, Jilin 130024, P. R. China.

E-mail: xinglong@nenu.edu.cn (X.-L. Wu)

^b School of Materials Science and Engineering, Nanyang Technological University, 50 Nanyang Avenue, Singapore 639798, Singapore. E-mail: alexyan@ntu.edu.sg (Q. Yan)

[§] D.L. and H.L. contributed equally

^{*} The corresponding authors

This supplementary information includes:

1. Experimental Section
2. Supplementary Fig. S1-S11
3. Supplemental References

1. Experimental Section

Preparation of reduced graphene oxide (RGO): Graphene oxide (GO) was firstly prepared from the modified Hummers method as previously reported.¹ RGO nanosheets can be further obtained by annealing GO powder in a high pure mixture atmosphere ($\text{H}_2:\text{Ar} = 5\%:95\%$, volume) at 1000 °C for 2 hours.

Preparation of the $(\text{Si}@\text{MnO})@\text{C}/\text{RGO}$ nanohybrid: Firstly, the solution of manganese oleate in n-hexane ($\text{Mn}(\text{oleate})_2/\text{n-hexane}$) was prepared through a replacement reaction between sodium oleate and manganese chloride (MnCl_2) and then extraction in the mixed solution of n-hexane/alcohol/water.² Secondly, in order to prepare the precursor solution for designed $(\text{Si}@\text{MnO})@\text{C}/\text{RGO}$, the commercial Si powder with average diameter of about 100 nm was further added into the obtained $\text{Mn}(\text{oleate})_2/\text{n-hexane}$ solution with the mole ratio of $\text{Si}:\text{Mn}(\text{oleate})_2 = 2.2:5$ under continuous stirring at room temperature for 3 hours. And then, the prepared RGO powder of 36 mg was further added into the above mixture followed by a sonication treatment of above 4 hours. Thirdly, the solvent of n-hexane in the precursor solution was removed on a rotavapor under vacuum at 70 °C, obtaining the solid precursor. Finally, the $(\text{Si}@\text{MnO})@\text{C}/\text{RGO}$ nanohybrid can be collected after annealing the solid precursor with a heating rate of 1 °C min^{-1} in the high purity nitrogen at 500 °C for 2 hours. Because the cycling stability is dependent on the ratio between Si and MnO according to the proposed strategy, we also prepared two contrast samples to optimize the properties. In the two controls, the molar ratio of $\text{Si}:\text{Mn}(\text{oleate})_2$ is 1.4:5 and 2.8:5, respectively. The cycling performances are compared in Fig. S5, disclosing that the sample prepared from mole ratio of $\text{Si}:\text{Mn}(\text{oleate})_2 = 2.2:5$ shows the best cycling stability in compared to two controls.

Preparation of the $\text{Si}@\text{RGO}$ comparative: The preparation processes are very similar with the above ones for $(\text{Si}@\text{MnO})@\text{C}/\text{RGO}$ preparation just without the usage of manganese oleate. Typically, 60 mg of commercial Si and prepared RGO powders were added into 50 mL n-hexane solution sequentially, and then followed by a sonication treatment of above 4

hours. After evaporating the solvent of n-hexane, Si@RGO can be collected after annealing the solid precursor with a heating rate of 1 °C min⁻¹ in the high purity nitrogen at 500 °C for 2 hours.

Preparation of the MnO@C/RGO comparative: The preparation processes are the same as the above-mentioned ones for the (Si@MnO)@C/RGO preparation just without the usage of commercial Si material.

Materials characterization: The composition of all samples were determined by X-ray powder diffraction (Bruker D8 ADVANCE diffractometer, $\lambda = 1.5406 \text{ \AA}$, Cu K α). The structure, morphology and size of all products were analyzed by scanning electron microscopy (10 kV, JEOL JSM-6700F field emission) and transmission electron microscopy (JEOL-2100 F, operated at 200 kV). Elemental mapping by energy-dispersive X-ray spectroscopy was used to investigate the distribution of all elements in the products. Raman spectrum was performed on a DXR Raman Microscope (Thermo Scientific) with a laser wavelength of 532 nm, which was first calibrated with a Si wafer (520 cm⁻¹). The N₂ adsorption/desorption isotherms were measured at 77.4 K with a Micromeritics ASAP 2020 analyzer. The pore-size distribution was fitted from desorption isotherm by using the Barrett-Joyner-Halenda (BJH) method. Thermogravimetric analyses (TGA, Q500 from TA Instruments) were carried out in air flow at a heating rate of 10 °C min⁻¹. The inductively coupled plasma atomic emission spectroscopy (ICP-AES) was obtained on Shimadzu, ICPS-8100.

Electrochemical measurements: The electrodes were prepared by coating a slurry of 80% active materials, 10 wt% polyvinylidene fluoride binder, and 10 wt% acetylene black in N-methyl-2-pyrrolidinone (NMP) upon the Cu or Al foils for anodes or cathodes respectively, which were thereafter dried under vacuum at 100 °C for above 12 hours to remove NMP. LiFePO₄ and LiNi_{0.6}Co_{0.2}Mn_{0.2}O₂ were purchased from Foshan Dynanonic Co., Ltd and ECOPRO Co., Ltd, respectively. CR2032 coin cells were fabricated in an Ar-filled glovebox

with concentrations of H₂O and O₂ below 0.1 ppm. Metallic Li was employed as the counter electrode for half cells. The loading mass of active materials on electrodes was about 2-2.5 mg cm⁻². The electrochemical properties of fabricated cells were tested under an atmospheric environment by using a multichannel battery (LAND CT2001A) measuring system. Cyclic voltammetry (CV) tests were performed on a VersaSTAT3 (Princeton Applied Research). Glass microfiber filters were employed as separators, and 1 mol L⁻¹ LiPF₆ in a mixture of ethylene carbonate (EC) and dimethyl carbonate (DEC) (v/v=1:1) was used as the electrolyte. The electrochemical performances of the full cells were also tested in a multichannel battery (LAND CT2001A) measuring system in the voltage windows of 1.0-3.8 V and 1.0-4.2 V for LiFePO₄ and LiNi_{0.6}Co_{0.2}Mn_{0.2}O₂ cathodes respectively. The specific capacities of full cells were calculated according to the mass of cathode materials.

2. Supplementary Fig. S1-S10

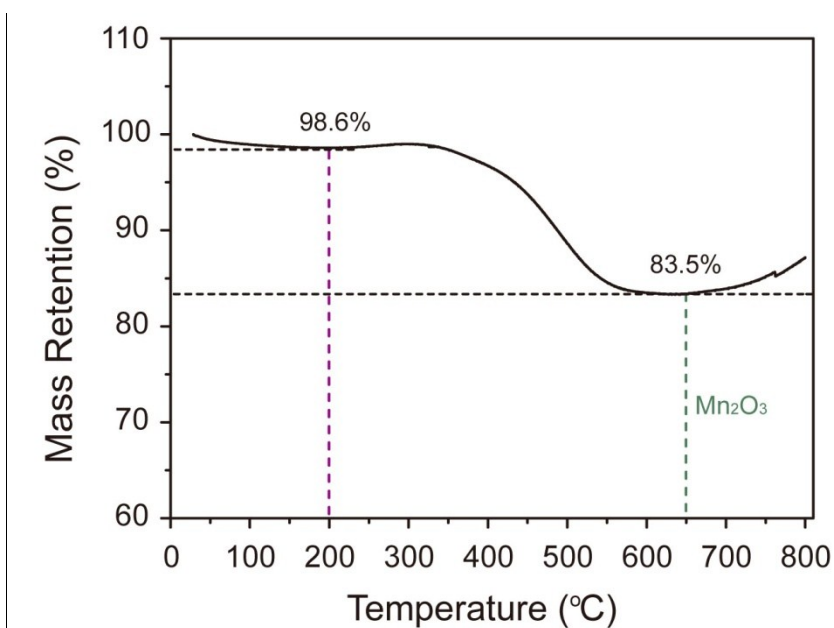


Fig. S1. Mass retention of the as-prepared (Si@MnO)@C/RGO by Thermogravimetric analysis. Temperature was scanned from room temperature to 800 °C, at a heating rate of 10 °C min⁻¹ under air atmosphere. Note that, The mass percent of MnO in (Si@MnO)@C/RGO is 39% by ICP-AES analysis. Combining the results obtained from the TGA, the mass ratio of Si:MnO:carbon are equal to 42:39:19 in (Si@MnO)@C/RGO.

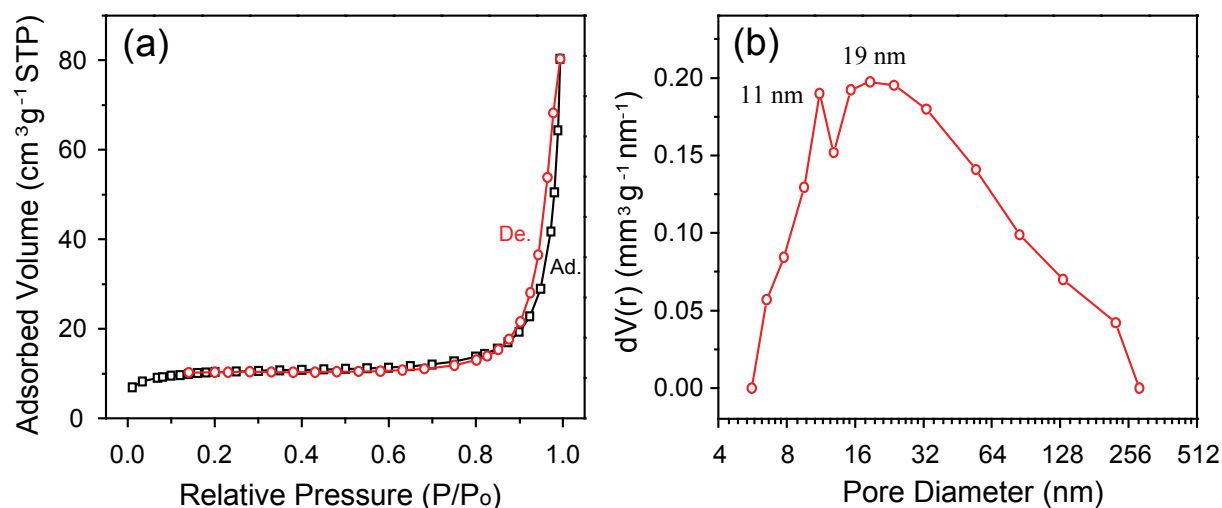


Fig. S2. (a) N₂ adsorption-desorption isotherm and (b) the corresponding BJH pore size distribution of the as-prepared (Si@MnO)@C/RGO.

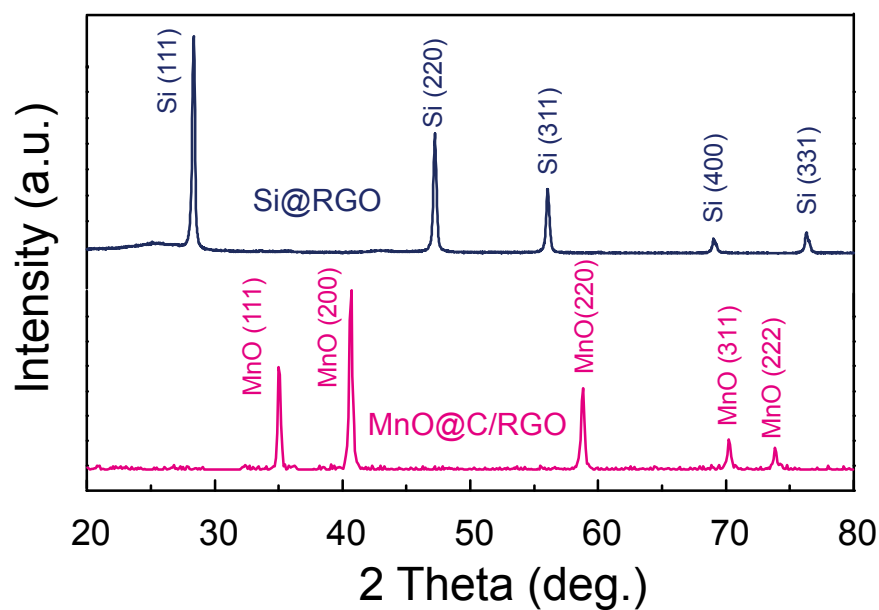


Fig. S3. XRD patterns of the Si@RGO and MnO@C/RGO comparatives.

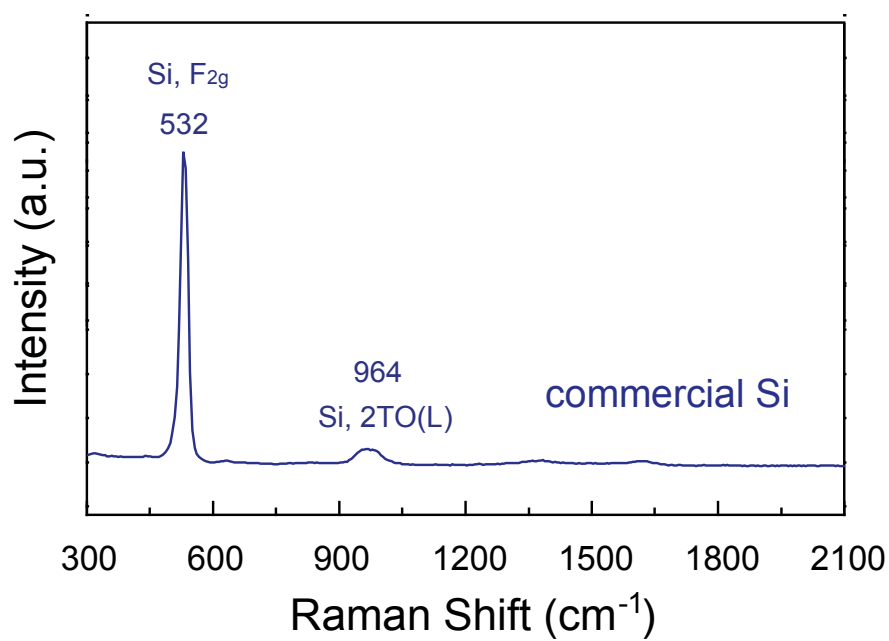


Fig. S4. Raman spectrum of the commerical Si material.

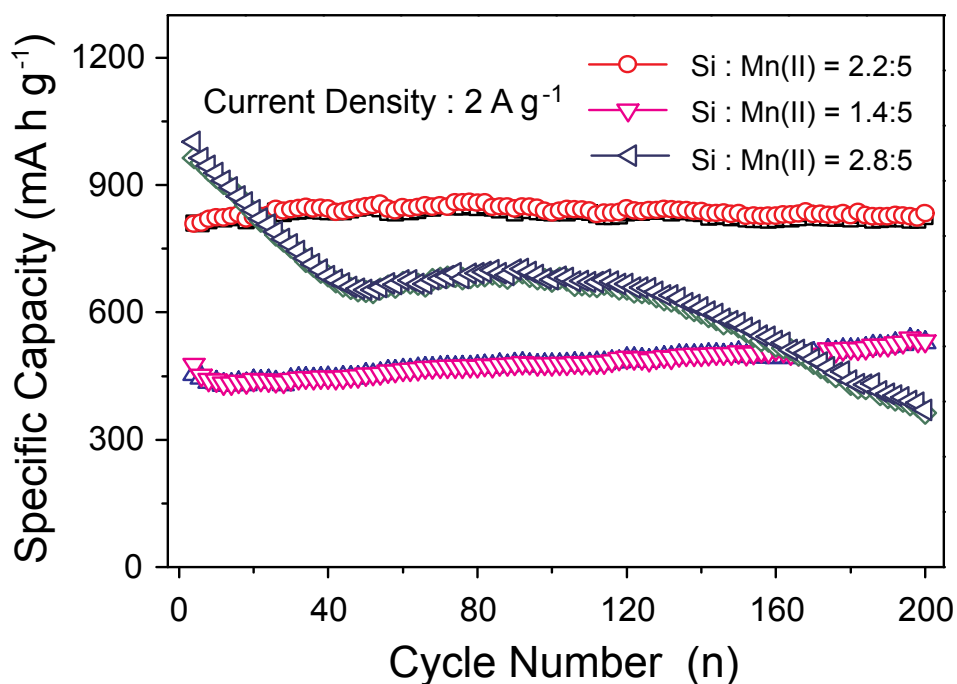


Fig. S5. The comparison of cycling performances for the (Si@MnO)@C/RGO hybrids prepared from different molar ratio between Si and Mn(oleate)₂, disclosing that the sample from the mole ratio of Si:Mn(oleate)₂ = 2.2:5 has the optimized cycling stability. Note that, in such sample, the mass ratio of Si, MnO and carbon is about 42:39:19, which is calculated from the results of ICP-AES and TGA.

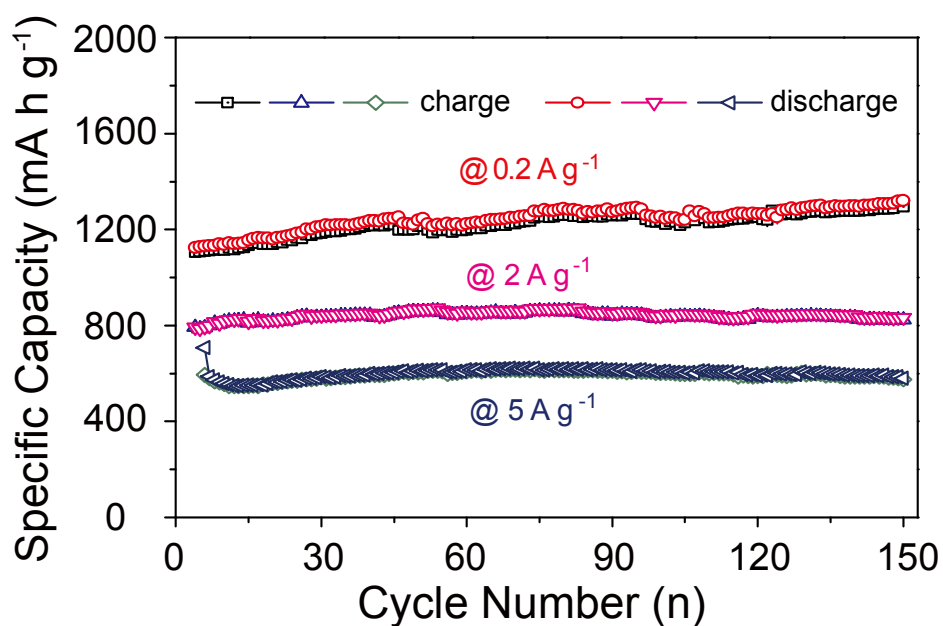


Fig. S6. Cycling performance of the prepared (Si@MnO)@C/RGO nanohybrid cycled at various current densities of 0.2, 2 and 5 A g⁻¹.

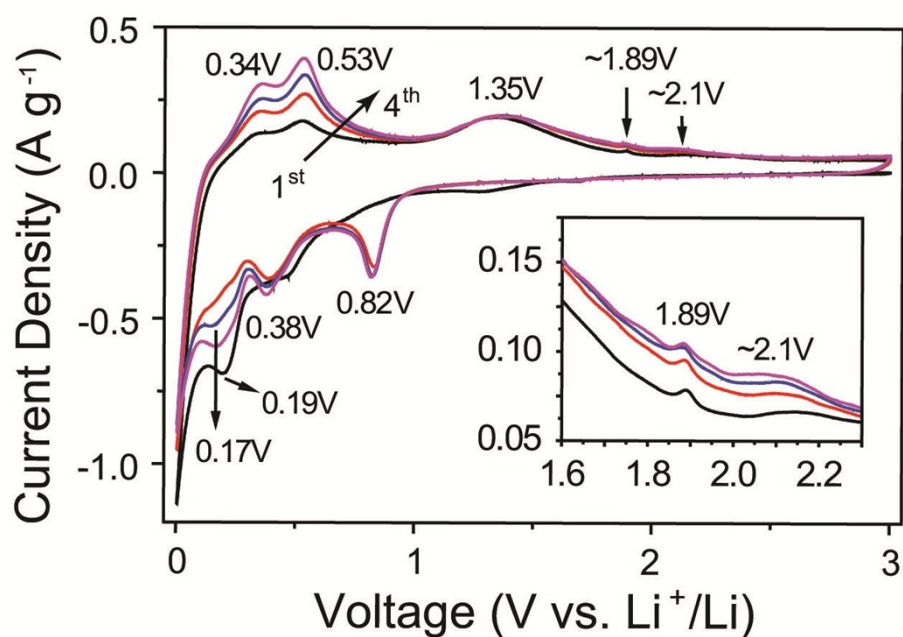


Fig. S7. CV curves of the (Si@MnO)@C/RGO with the optimized constituents at a scan rate of 0.1 mV s^{-1} in the voltage range of 0.005-3 V.

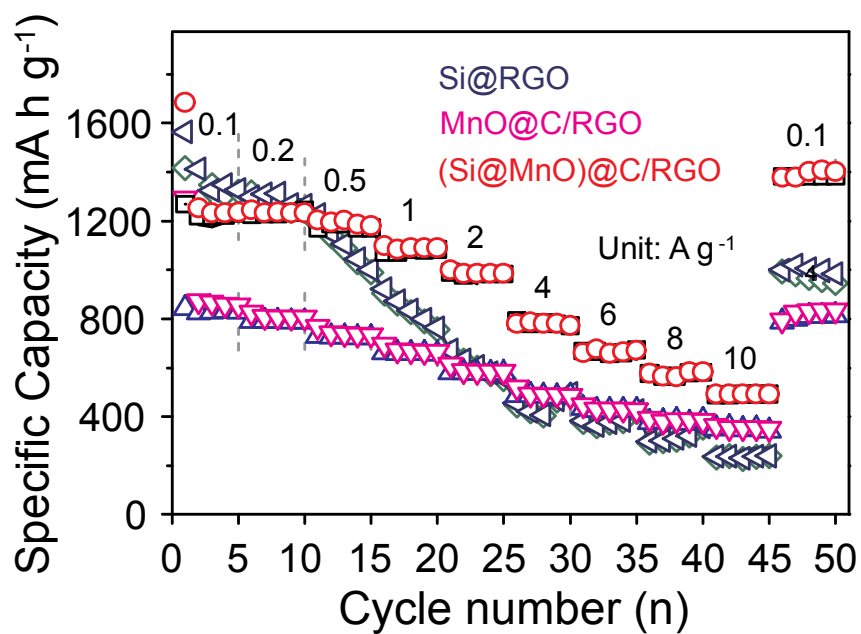


Fig. S8. The comparison of rate performance from 0.1 A g^{-1} to 10 A g^{-1} between all three products.

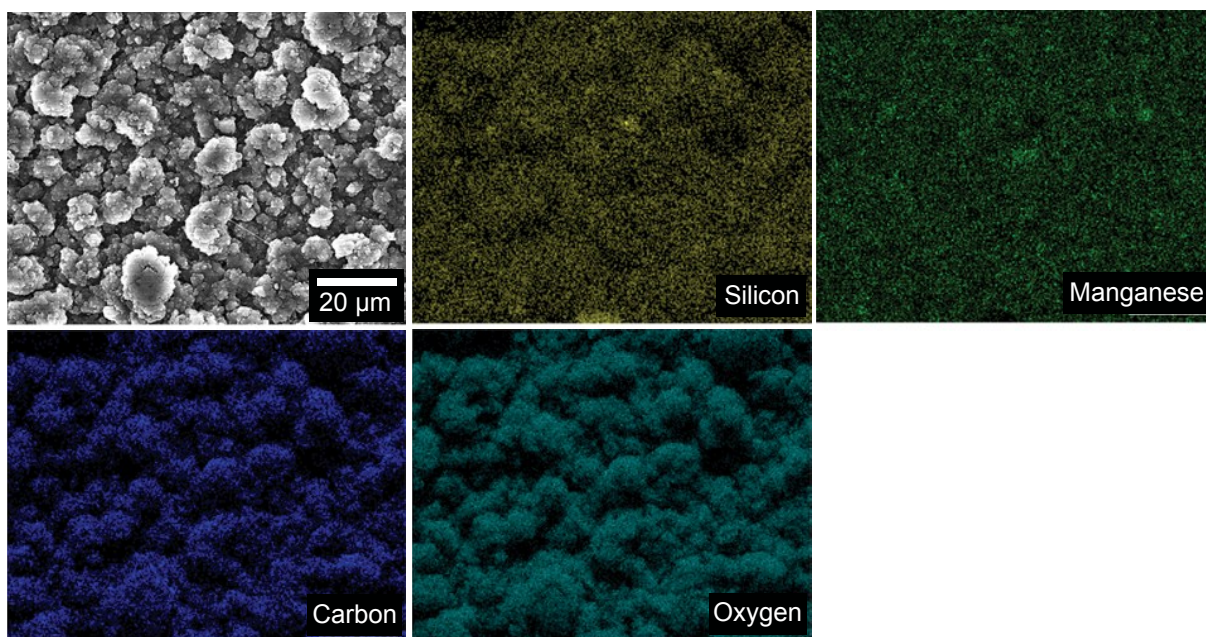


Fig. S9. SEM image and the corresponding EDX elemental mapping of silicon, manganese, carbon and oxygen elements of the (Si@MnO)@C/RGO electrode after 200 cycles at 3 A g⁻¹.

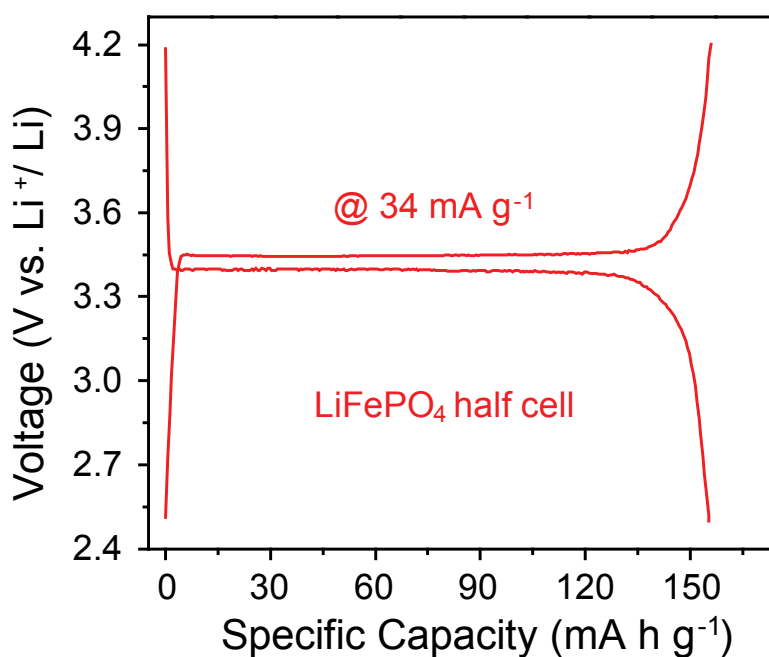


Fig. S10. Galvanostatic curve of commercial LiFePO₄ cathode in the half cell cycled at 2.5-4.2 V vs. Li⁺/Li.

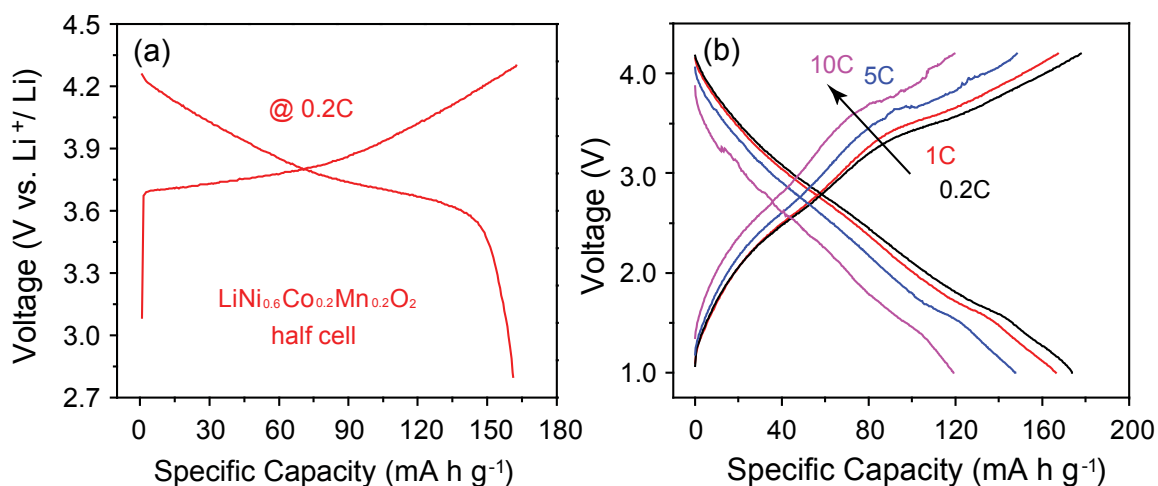


Fig. S11. (a) Galvanostatic curve of commercial $\text{LiNi}_{0.6}\text{Co}_{0.2}\text{Mn}_{0.2}$ cathode in half cell cycled at 2.8-4.3 V vs. Li^+/Li . (b) Galvanostatic curves of the fabricated $(\text{Si}@\text{MnO})@\text{C}/\text{RGO} // \text{LiNi}_{0.6}\text{Co}_{0.2}\text{Mn}_{0.2}\text{O}_2$ full cell cycled at 1.0-4.2 V at various rates from 0.2C to 10C.

3. Supplemental References

- 1 W. S. Hummers and R. E. Offeman, *J. Am. Chem. Soc.*, 1958, **80**, 1339.
- 2 J. Park, K. An, Y. Hwang, J. G. Park, H. J. Noh, J. Y. Kim, J. H. Park, N. M. Hwang and T. Hyeon, *Nat. Mater.*, 2004, **3**, 891-895.